Relaxation processes of water in the liquid to glassy states of water mixtures studied by

broadband dielectric spectroscopy

Relaxation processes of water in the liquid to glassy states of water mixtures studied by broadband dielectric spectroscopy

N Shinyashiki[1,3]**, S Sudo**[1]**, S Yagihara**[1]**, A Spanoudaki**[2]**, A Kyritsis**[2] **and P Pissis**[2]

[1] Department of Physics, Tokai University, Hiratsuka, Kanagawa 259-1292, Japan
[2] Department of Physics, National Technical University of Athens, Zografou Campus, 15780 Athens, Greece

E-mail: naoki-ko@keyaki.cc.u-tokai.ac.jp

Abstract

The relaxation processes of water mixtures of glycerol, ethylene glycol, ethylene glycol oligomers with two to six repeat units, poly(ethylene glycol) 400 and 600, fructose, and propanol have been studied by broadband dielectric spectroscopy at different water contents in the frequency range 10 μHz–20 GHz and in the temperature range 300–80 K without water crystallization. The results show that, in the vicinity of the glass transition temperature of the mixtures, two kinds of water exist. Part of the water behaves as excess water retaining its inherent mobility and appearing as a separate relaxation process (named here the ν-process) at frequencies higher than the structural α-process at subzero temperatures. Another part of the water moves cooperatively with solute molecules and contributes to the α-process.

(Some figures in this article are in colour only in the electronic version)

1. Introduction

The drastic change of dynamics of molecules in non-crystallizable materials, i.e., glass formers, during the transition from the liquid to the glassy state has attracted much attention, and various kinds of phenomena have been discovered. Dielectric measurements offer the advantage of providing precise data over a remarkably wide frequency range. Usually, in the liquid state, at temperatures well above the glass transition, only one dielectric relaxation process appears in the GHz frequency range. The process shifts to lower frequency with decreasing temperature, and in many cases at a splitting temperature, T_S, separates into two distinct

---

[3] Author to whom any correspondence should be addressed.

processes named α and β in order of increasing frequency. The α-process is the primary, structural relaxation related to the glass transition. Comparing the thermal glass transition temperature observed by differential scanning calorimetry (DSC) and the dynamics observed by dielectric measurements, it has been found that the glass transition occurs when the relaxation time of the α-process, τ_α, is in the range between 1 and 100 s [1–5]. The temperature dependence of τ_α obeys the Vogel–Fulcher (VF) law [6, 7],

$$\tau = \tau_{\infty,\text{VF}} \exp\left(\frac{A}{T - T_0}\right), \tag{1}$$

where $\tau_{\infty\text{VF}}$, A, and T_0 are empirical parameters.

The asymmetric loss peak of the α-process has been described by the Davidson–Cole [8] or the Kohlrausch–Williams–Watts (KWW) [9, 10] equation:

$$\Phi(t) = \exp[-(t/\tau_\text{K})^{\beta_\text{K}}], \tag{2}$$

where τ_K is the relaxation time and β_K is an asymmetric broadening parameter. The non-Debye and non-Arrhenius properties of the α-process are attributed to its cooperative nature.

Below T_g the temperature dependence of the relaxation time of the secondary β-process obeys the Arrhenius law,

$$\tau = \tau_\infty \exp\frac{\Delta E}{kT}, \tag{3}$$

where τ_∞ is the pre-exponential factor, ΔE is an apparent activation energy and k is the Boltzmann constant. Its broad and symmetric loss peak is described by the Cole–Cole equation [11]. Ngai *et al* proposed [12] that in many cases the β-process can be attributed to non-cooperative motions of essentially all parts of the molecule, classified as the Johari–Goldstein (JG) process [13, 14]. The JG process is observed even for glass-forming liquids without any intramolecular degrees of freedom (rigid molecules) and it can be considered as a precursor or local step that eventually leads to the structural α-process [12]. It has been shown that the primitive relaxation time, τ_0, is located near the most probable relaxation time, τ_JG, of the JG relaxation. τ_0 ($\sim\tau_\text{JG}$) is a function of the relaxation time of the α-process, τ_α, and the coupling constant, n, given by [15],

$$\tau_0 = t_\text{c}^n \tau_\alpha^{1-n}, \tag{4}$$

where $t_\text{c} =$ is a crossover time that has the approximate value of 2 ps for small molecular liquids [15]. The coupling constant, n, is related to the stretch exponent of the Kohlrausch function, β_K, as $n = 1 - \beta_\text{K}$ [15]. We can regard τ_0 obtained by equation (4) as τ_JG. Any additional higher-frequency processes are attributed to local motions, have no connection to the α-process and are expected to be less relevant to glass transition phenomena [12].

Recently, binary and ternary systems have been the object of such kind of studies. In particular, mixtures of water have been investigated extensively. We have carried out systematic broadband dielectric measurements of water mixtures, with various water contents and molecular structure of solute, in the temperature range 120–300 K and in the frequency range 10 μHz–20 GHz. Ethylene glycol [16], glycerol [17], ethylene glycol oligomer (EGO) with various numbers of repeat units [18–20], and fructose [21] were used as solutes. For each mixture, a single loss peak was observed above T_S, while the primary α and secondary processes were observed below T_S. The α-process is due to the cooperative motion of water and solute molecules and is related to the thermal glass transition of the mixture. The secondary process appearing at the high-frequency side of the α-process is due to the local motion of non-crystallized water in sub-zero temperatures. The water molecules contributing to this process do not move cooperatively with solute molecules and seem to have the intrinsic mobility of water.

Therefore, this process is hereafter named the ν-process (from the initial of the word '$\nu\varepsilon\rho o$', meaning 'water' in modern greek). Similar conclusions were also drawn from the investigations of the water mixtures with *n*-propylene glycol (*n*PG: $n = 2, 3$) [22], tripropylene glycol [5], glucose [23], poly(ethylene glycol) (PEG) [23], and poly(vinyl pyrrolidone) (PVP) [23]. A special case are propanol–water mixtures [24], in which the ν-process appears at a frequency lower than that of the α-process, since T_g of propanol is lower than that of pure water.

In order to clarify the characteristic properties of the ν-process, we have conducted dielectric measurements of triethylene glycol (3EG)–water mixtures with various concentrations and compared the results with those of the literature [16–21, 24].

2. Experimental details

The 3EG used in these experiments was purchased from Aldrich. Water mixtures of 65, 70, 80, 90, 94, and 100 wt% concentration in 3EG were prepared. Distilled and deionized water with electric conductivity lower than 18.3 μS m^{-1} was obtained from an ultra-pure water distiller (Millipore, MILLI-Q Lab).

Complex permittivity was measured in the frequency range 10 μHz to 20 GHz and in the temperature range between 78 and 300 K. We used five measuring systems in order to cover this wide frequency range. From 100 MHz to 20 GHz, time domain reflectometry (TDR) method was employed. An RF impedance/material analyser (HP 4291A) was used between 1 MHz and 1.8 GHz and an LCR meter (HP 4284A) between 20 Hz and 1 MHz. From 2 mHz to 1 kHz and from 10 μHz to 10 mHz an AC phase analysis (ACPA) and DC transient current (DCTC) method were employed, respectively. Details of the equipments and procedures are reported in previous papers [16–20].

The results are compared to data on pure glycerol and 60, 65, 70 and 80 wt% glycerol–water mixtures [17], as well as on 60, 70, and 80 wt% ethylene glycol–water mixtures [16], pure 1-propanol and 80 wt% propanol–water mixture [24], 65 wt% di-, tetra-, penta- and hexaethylene glycol–water mixtures [18, 19], 65 wt% PEG400- and PEG600-water mixtures [20] and 94.6, 88.2, 86.5, 77.8 wt% fructose–water mixtures [21] from previous works. No water crystallization was observed in any of these systems.

3. Results and discussion

Figure 1 shows the dielectric losses for pure 3EG and 65 wt% 3EG–water mixture at various temperatures. Above 203 K for pure 3EG and 206 K for the mixture a single loss peak is observed. The peak shifts to lower frequencies with decreasing temperature. Two or three relaxation processes are observed at low temperatures. For pure 3EG the primary α-process and the secondary β-process are observed, as shown in figure 1(b). For the 65 wt% 3EG–water mixture, the ν-process, whose strength is much larger than that of the β-process observed for pure 3EG, appears at the high-frequency side of the α-process (figure 1(d)). At the high-frequency side of the ν-process, there is a contribution of an excess wing or a high-frequency flank of another relaxation process (figure 1(d)).

The complex permittivity of 3EG–water mixture can be described by

$$\varepsilon(\omega) = \varepsilon' - j\varepsilon'' = \varepsilon_\infty + \sum_i \frac{\Delta\varepsilon_i}{1 + (j\omega\tau_i)^{\beta_{CC_i}}} + \Delta\varepsilon_a \int_0^\infty \left(-\frac{d\Phi(t)}{dt}\right) \exp(-j\omega t)\,dt$$
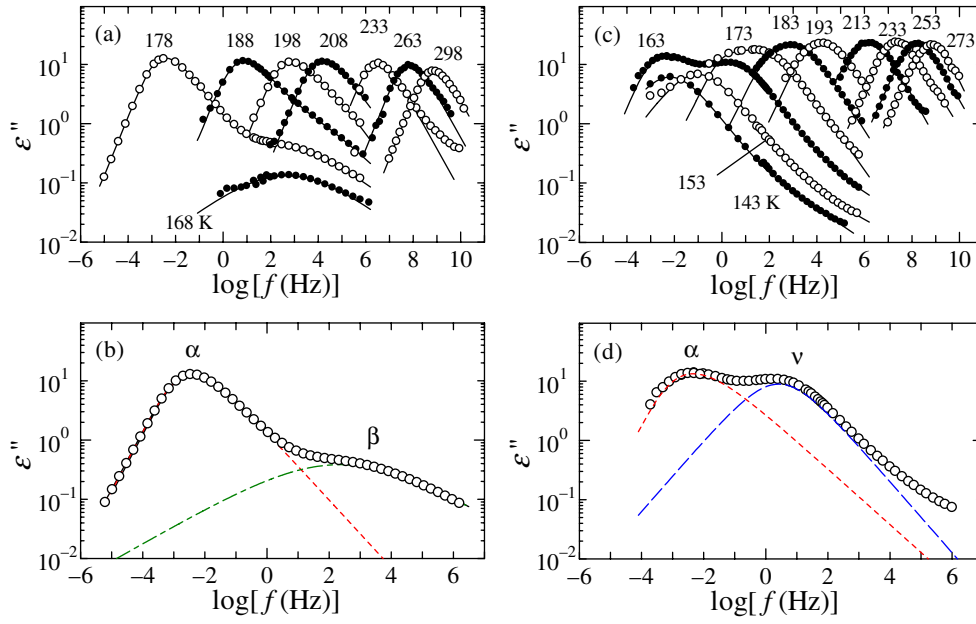$$- j\frac{\sigma}{\omega\varepsilon_0}. \tag{5}$$

Figure 1. Dielectric losses for left: triethylene glycol (a) at various temperatures and (b) at 178 K, and right: 65 wt% triethylene glycol–water mixture (c) at various temperatures and (d) at 163 K. The dotted lines are fits to the Kohlrausch–Williams–Watts function and the dashed line and dotted–dashed line are fits to the Cole–Cole equation.

Here, ω is the angular frequency, ε_∞ is the high-frequency limit permittivity, $\Delta\varepsilon$ is the relaxation strength, τ is the relaxation time, β_{CC} is a symmetric broadening parameter ($0 < \beta_{CC} \leqslant 1$), t is the time, j is the imaginary unit, σ is the dc conductivity and ε_0 is the vacuum permittivity. The second term of the right-hand side of equation (5) is the summation of Cole–Cole equations [11] and the subscript i indicates the relaxation processes (ν or β). The third term describes the α-process by a KWW function (equation (2)). The fourth term is the contribution of dc conductivity. The relaxation time of the α-process was obtained from the loss peak maximum frequency, f_m, as $\tau_\alpha = 1/2\pi f_{m,\alpha}$. In the following, we define the dielectric glass transition temperature, T_g, as the temperature at which τ_α is 100 s.

Figures 2 and 3 show the temperature dependences of the relaxation times, τ, and relaxation strengths, $\Delta\varepsilon$, of the relaxation processes observed for pure 3EG and 65 wt% 3EG–water mixture. For pure 3EG, the temperature dependence of τ_α can be described by the VF law (equation (1)). On the other hand, the temperature dependence of the relaxation time of the β-process obeys the Arrhenius law (equation (3)). The relaxation strength of the α-process increases monotonically with decreasing temperature while that of the β-process is less than 5% of that of the α-process. Accordingly, the relaxation time and strength of the β-process cannot be reliably determined above T_g. In the temperature range between T_S and T_g the β-process is neglected during the fitting procedure. Due to its small strength this does not affect considerably the results for the α-process.

In the spectrum of the 65 wt% 3EG–water mixture, the ν-process appears at frequencies higher than the α-process. The traces of relaxation time and relaxation strength at high temperatures continue to those of the ν-process and the α-process seems to appear at $T_S = 206$ K. Taking into consideration the relaxation strength of pure 3EG and pure water at 25 °C, the contribution of water to the relaxation strength at this temperature should be two times
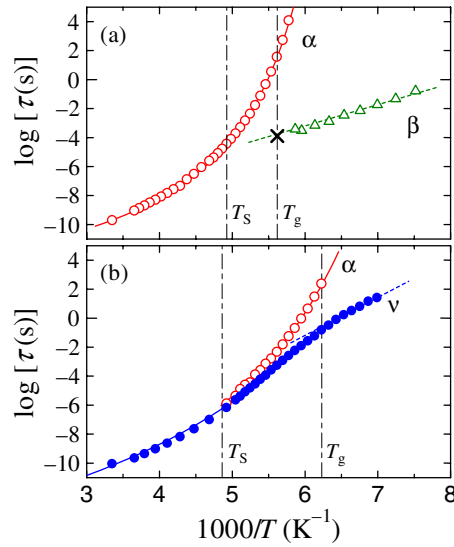
4

Figure 2. Temperature dependence of the dielectric relaxation time τ for (a) 3EG and (b) 65 wt% 3EG–water mixture. Open circles, filled circles, and open triangles indicate the relaxation time of the α-, ν-, and β-processes, respectively. The cross indicates the Johari–Goldstein relaxation time; τ_{JG} was calculated using equation (4) with $\beta_K = 0.58$ of the α-process at T_g i.e., $\tau_\alpha = 100$ s obtained by fitting the α-peak of the dielectric spectra.
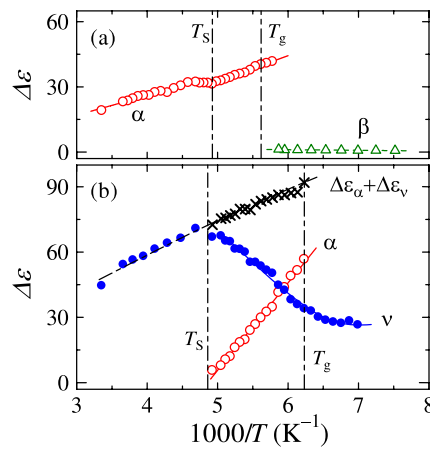

Figure 3. Temperature dependence of the dielectric relaxation strength $\Delta\varepsilon$ for (a) 3EG and (b) 65 wt% 3EG–water mixture. Open circles, filled circles and open triangles indicate the relaxation strength of the α-, ν-, and β-processes, respectively. Crosses indicate the sum of the relaxation strengths of the α-process $\Delta\varepsilon_\alpha$ and the ν-process $\Delta\varepsilon_\nu$.

larger than that of 3EG. In other words, the ν-process is dominant above T_S. In the mixture, the sum $\Delta\varepsilon_\alpha + \Delta\varepsilon_\nu$ of the relaxation strengths of α and ν monotonically increases with decreasing temperature and its extrapolation agrees well with the dielectric strength above T_S. At temperatures between T_S and T_g, $\Delta\varepsilon_\alpha$ increases and $\Delta\varepsilon_\nu$ decreases with decreasing temperature. This implies that the water molecules contributing to the ν-process change to contributing to the α-process: as the temperature decreases, the increase in the cooperativity

of the molecular motion contributing the α-process leads more water molecules to join the α-process from the ν-process.

The relaxation time of the ν-process obeys the VF law above T_g and the Arrhenius law below T_g. This change should be related with the difference between the relaxation time of the α- and ν-processes. In the temperature range between T_S and T_g, the loss peak of the α- and ν-processes can be distinguished, but the high-frequency flank of the α-process and the low-frequency flank of the ν-process fully overlap. Then the time scales of a part of motions contributing the α- and ν-processes is the same and correlation of these two processes can be expected. Below T_g the molecular motion contributing the α-process freezes and the ν-process loses the correlation with the α-process and shows an Arrhenius temperature dependence. The change from the VF to Arrhenius dependence of τ_ν does not appear in the water mixtures with fructose [21], ethylene glycol [16] and glycerol [17]. For the fructose–water mixtures, the α- and ν-processes separate in the liquid state, in which the correlation between the α- and ν-processes is weak and the difference between τ_ν and τ_α is large just above T_g, so that only the Arrhenius dependence of τ_ν can be seen. For the water mixtures with ethylene glycol and glycerol, the difference between τ_α and τ_ν is small in the temperature range measured. It is expected that the temperature dependence of τ_ν becomes weaker at low temperatures. The change from the VF to Arrhenius dependence is observed not only for various water mixtures [5, 18–20, 22, 23] but also generally for the JG process [12]. This behaviour seems to be common to some kinds of non-cooperative secondary processes. Further investigation would be necessary for a deeper understanding of this phenomenon.

In order to characterize the β-process observed for pure 3EG, its relaxation time, τ_β, was compared to the relaxation time of the JG process, $\tau_{JG} = 0.18$ ms, estimated according to the coupling model (equation (4)), using the values τ_α 100 s, $\beta_K = 0.58$, and $t_c = 2$ ps at T_g. The result is represented by the cross in figure 2. For pure 3EG, τ_{JG} agrees well with τ_β. According to the criterion given by equation (4), it is possible to say that the β-process of pure 3EG is the Johari–Goldstein process. In contrast, the secondary process observed at ambient pressure for the propylene glycol oligomer, whose molecular structure is similar to 3EG, is not the JG process judging by the same criterion [12, 25]. Further studies, for example of the pressure dependence, are necessary for the attribution of the β-process of pure 3EG. For 65 wt% 3EG– water mixture the higher-frequency side of the ν-process can be described by assuming another process, but the relaxation time of this process obtained in this way is inaccurate. Such an excess wing, i.e., high-frequency flank of the relaxation process appears also for the water mixtures of ethylene glycol [16], glycerol [17], and other EGOs [18–20]. It seems to be a kind of common property of water mixtures, but further studies are necessary for understanding it.

Figure 4 shows plots of the relaxation strength and relaxation time of the relaxation processes in the 3EG–water mixture at 178 K against mole fraction of water, X_W. The relaxation times of the α- and ν-processes decrease with increasing water content, this dependence being stronger above $X_W = 0.6$. The relaxation strength of the α-process increases with increasing X_W up to $X_W = 0.6$. This means that the molecular motion of water molecules contributes to the α-process. In this concentration range, the strength of the ν-process is negligibly small or vanishes. Therefore, at water contents below $X_W = 0.6$, most of the water molecules move cooperatively with 3EG molecules. For water contents above $X_W = 0.6$, the strength of the α-process decreases with increasing X_W. The ν-process appears at about $X_W = 0.6$ and increases with increasing X_W. If the mixture contains excess water, the excess water molecules cannot move cooperatively with 3EG molecules and they start to contribute to the ν-process. Although the ν-process is mainly due to the excess water, its relaxation time is influenced by that of the α-process. The sum of the relaxation strengths of the α- and ν- processes, $\Delta\varepsilon_\alpha + \Delta\varepsilon_\nu$, increases monotonically with increasing X_W and agrees well with the
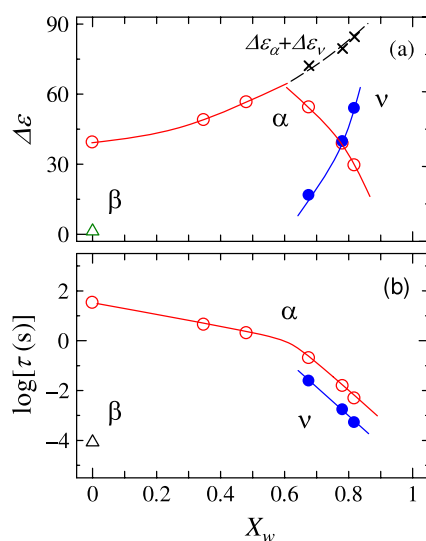
Figure 4. Plots of the dielectric (a) relaxation strength $\Delta\varepsilon$ and (b) relaxation time τ against mole fraction of water X_W for 3EG–water mixtures at 178 K. Open circles, filled circles, and open triangles indicate the relaxation strength $\Delta\varepsilon$ and the relaxation time τ of the α-, ν-, and β-processes, respectively. Crosses indicate the sum of the relaxation strengths of the α-process $\Delta\varepsilon_\alpha$ and the ν-process $\Delta\varepsilon_\nu$.

extrapolation of the strength of the α-process below $X_W = 0.6$. For the water mixtures with glycerol [17], nPG [22], and tripropylene glycol [5], the strength of the ν-process increases abruptly or the process seems to appear around $X_W = 0.6$–0.7, i.e. in the same concentration range as in the 3EG–water mixtures.

From the X_W dependence of the α-process, we can estimate that less than two water molecules can move cooperatively with one 3EG molecule. These water molecules are included in the cooperatively rearranging region (CRR) [26] of 3EG molecules. Depending on its size and structure each solute molecule has a capacity of water molecules which move cooperatively with it. The temperature dependence of the $\Delta\varepsilon_\alpha$ and $\Delta\varepsilon_\nu$ (figure 3) shows that this capacity increases with decreasing temperature.

Figure 5 shows schematically the α- and ν-processes depending on the molecular size of EGO observed for 65 wt% EGO–water mixtures reported previously [18–20, 27]. At this concentration, the contribution of dipole moments of water to the relaxation strength is larger than that of EGO. The left-hand side of the figure corresponds to water mixture with small EGO molecules (ethylene glycol and diethylene glycol), while the right-hand side corresponds to those with large EGO molecules (triethylene glycol and longer EGO chain). In the case of the small-EGO–water mixtures, the shape of the primary dielectric loss peak is asymmetrical above the splitting temperature, T_S, at which the separation of the α- and ν-processes occurs. Below T_S the asymmetric process continues as the α-process and the ν-process follow a separate trace at higher frequency. In contrast, the large-EGO–water mixtures show a broad and symmetrical loss peak above T_S. The symmetric loss peak continues as the ν-process, while the α-process exhibits an onset at T_S. These different patterns of the α–ν separation correlated with the shape of the loss peak above T_S are the result of the differences in the cooperativity of water and solute molecules: the cooperative motion of water and solute molecules leads in the case of small-EGO–water mixtures to the common asymmetric peak above T_S. In contrast, for the
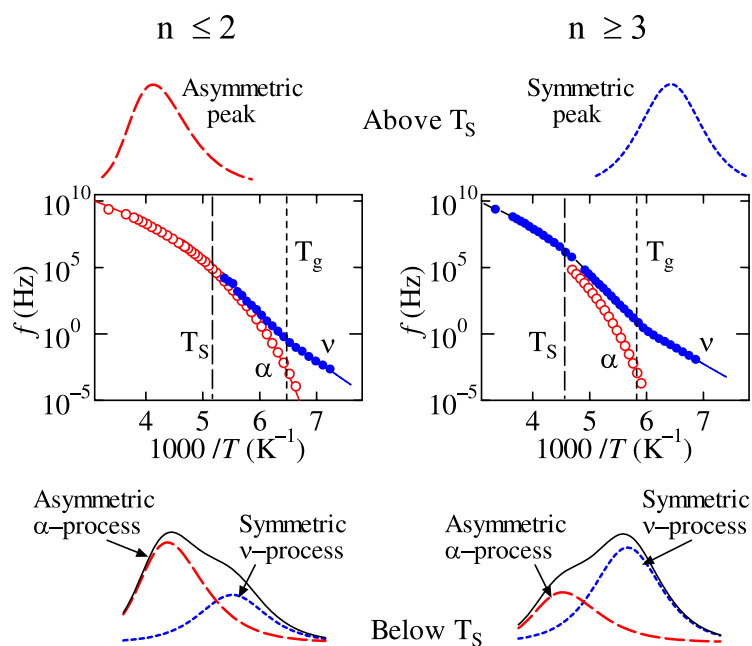
Figure 5. Schematic representations of the relaxation processes observed for 65 wt% ethylene glycol oligomer–water mixtures with small number of repeat units of EGO, n, ($n \leqslant 2$) at the left-hand side, and large $n (n \geqslant 3)$ at the right-hand side. Top: dielectric loss peaks above T_S. Bottom: dielectric loss peaks below T_S. Middle: temperature dependence of loss peak frequencies, f, of the α- and ν-processes.

large-EGO–water mixture the spatially restricted local motion of water molecules leads to the symmetric loss peak above T_S. It is noted that the separation below T_S of the α- and ν-processes for small-solute–water mixtures is the decoupling of the motions of water and solute molecules, and that for large-solute–water mixtures is the coupling of the motions of solute and a part of water molecules. The relaxation time of the α-process depends strongly on the EGO molecular size [19]. On the other hand, the relaxation time of the ν-process has weak solute molecular size dependence for an EGO larger than triethylene glycol [19].

Figure 6 shows the dielectric loss spectrum of the 80 wt% propanol–water mixture [24]. The three relaxation processes, I, II (the structural relaxation) and III, observed for pure propanol are also present in the mixture, with almost the same frequencies [24]. An additional relaxation process is observed at frequencies lower than I. At high temperatures, when the mixture is in the liquid state, process I and the additional low-frequency process are unified in one single loss peak. With decreasing temperature, it shifts to lower frequencies and separates into two peaks. According to the temperature and concentration dependences of the relaxation strength, the lowest-frequency process is due to the molecular motion of water in the propanol–water mixture [24], i.e., the ν-process. The fact that ν-process appears at a frequency lower than that of the primary process for propanol–water mixtures, opposite to what is the case for the other solutes studied, is expected, if we consider the relation between the glass transition temperatures of water and solute. The glass transition temperature of the studied solutes is higher than the glass transition temperature of pure water, 136 K [28], while the T_g of pure propanol is 95.9 K [24], lower than that of pure water. In other words in the case of propanol, the relaxation process of excess water is slower than the α-process of the solute.
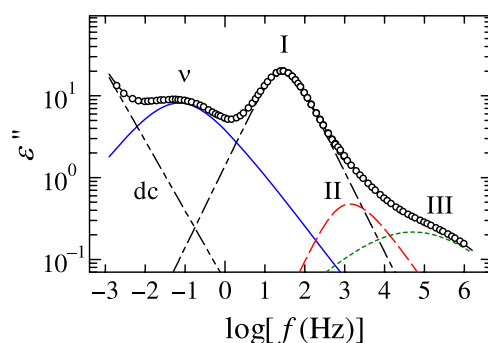
Figure 6. Frequency dependence of dielectric loss for 80 wt% propanol–water mixture at 123 K. The lines were obtained by curve fitting with three Cole–Cole processes (solid line: ν-process, dotted line: process III, dot–dashed line: process I), one KWW process (dashed line: process II) and the contribution of dc conductivity (two dots–dashed line).

The glass transition temperature T_g of the water mixtures depends on the molecular structure of the solute and on the concentration. For the water mixtures we investigated T_g is in the range 90–270 K. T_g of the fructose–water mixtures is high relative to the other studied mixtures and the ν-process lies accordingly at higher temperatures [21]. The relaxation time of the ν-process also depends on the concentration and the molecular structure of the solute. Nevertheless, this dependence is not strong. Measurements on various kinds of water mixtures, such as water mixtures with tripropylene glycol [5, 22], dipropylene glycol [5], poly(ethylene glycol) [23], glucose [23], poly(vinyl pyrrolidone) [23], and poly(hydroxyl ethyl methacrylate) [29–31], and 2D layered water [32], have shown that the relaxation time of the ν-process remains in a limited area of the Arrhenius plane. This reinforces the claim that the ν-process is a manifestation of the inherent mobility of water at subzero temperatures.

In order to characterize the relationship between the relaxation times of the ν- and α-processes, the loss peak frequency of the ν- and β-processes at the glass transition temperature f_m $(T = T_g)$ were plotted against T_g (figure 7). The concentrations, values of T_g, and f_m $(T = T_g)$ for all the mixtures are listed in table 1. At T_g, the loss peak frequency of the α-process, $f_{m\alpha}(T = T_g)$, is 1.5 mHz ($f_m = 1/2\pi\tau_\alpha$). The differences between 1.5 mHz and f_m $(T = T_g)$ have the same physical content as the degree of separation between the ν-process and α-process at T_g.

The mixtures with higher T_g have higher values of f_m $(T = T_g)$ and the plot is restricted to the area between the dotted and dashed lines. The dashed line was drawn through the plots of the loss peak frequency of pure water at 273.35 K [33], which is the vicinity of the melting temperature of pure water, given by the double circle, and f_m $(T = T_g)$ of 80 wt% propanol water mixture. The dotted line was drawn through the plots of 94.6 wt% fructose–water mixture and 80 wt% 3EG–water mixture. The dotted line indicates that in the frequencies below the line, no loss peak of the ν-process appears for any water mixtures we measured. Within the coupling model the degree of frequency separation between the α- and JG processes, in other words f_m $(T = T_g)$ of the JG process, depends only on the coupling constant $n(=1 - \beta_K)$ [12]. n is independent of the glass transition temperature but depends on the fragility of the α-process [34–36]. In contrast to the JG process, f_m $(T = T_g)$ of the ν-process appears to vary with T_g. This results from the fact that the ν-process appears within a limited area on the Arrhenius plane, i.e. does not depend on the structure and concentration of the solute as strongly as T_g. Therefore, the frequency separation of α and ν differs depending on the solute
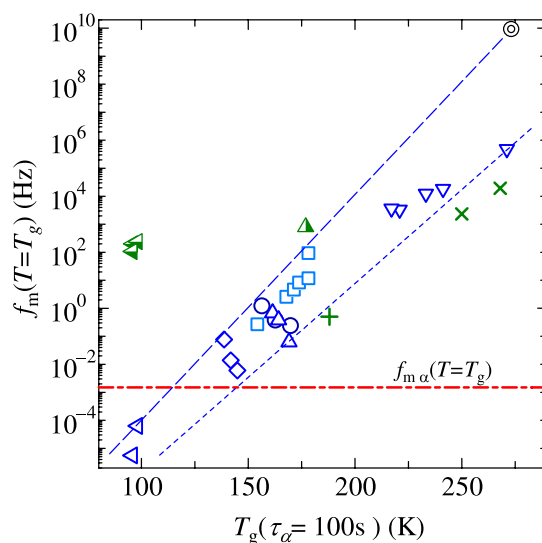
Figure 7. Plot of the loss peak frequency at T_g, f_m ($T = T_g$) of the ν-process (open symbols) and β-process (half-filled symbols) against dielectric T_g ($\tau_\alpha = 100$ s). Different shapes stand for the different solutes of water mixtures: left directed triangles, propanol; diamonds, ethylene glycol; circles, glycerol; upward triangles, 3EG; downward triangles, fructose; squares, ethylene glycol oligomers (EGOs). EGO–water mixtures are 65 wt% EGO with various size of EGO and other water mixtures are various concentrations. All the data are listed in table 1. Crosses are the Johari–Goldstein (JG) process of sorbitol and xylitol from Döß *et al* [37] and plus is the JG process of glycerol from Ngai *et al* [38]. The double circle is the loss peak frequency of water at +0.2 °C [33].

and concentration. The ν-process shows in this respect a completely different character than the JG process.

For water mixtures with small water content, the dielectric strength of the ν-process is small or even negligible, so it is difficult to distinguish the ν-process from the α-process. In this case, most of the water molecules contribute to the α-process and move cooperatively with the solute molecules. This means that the loss peak concerned with the water is on the dot–dashed line of 1.5 mHz in figure 7. If the mixture contains excess water which contributes to the ν-process, the frequency of the loss peak of excess water is shown by the plots. Adding water to the mixture, the mobility of water contributing to the ν-process becomes higher and the loss peak of the ν-process shifts to higher frequency. As the water concentration, and therefore mobility, becomes higher, the peak crosses finally the dashed line and moves to the upper side of the dashed line. The mobility of water is then sufficient to construct ice crystals within the time of the experiment and the excess water in the mixture crystallizes. Therefore, the dashed line can be considered as both the temperature and mobility (frequency) limit of water in a liquid state at subzero temperatures. The dashed line also indicates that the crystallization of water in the mixture is related to the glass transition temperature: the diffusive motion of molecules and consequently the time needed to form an ice crystal of excess water is related to the structural α-process and thus T_g. Therefore, both the time scale of the mixture α-process and the mobility of water molecules contributing to the ν-process determines whether the mixture is crystallized or not at subzero temperatures.

The f_m ($T = T_g$) values of the JG process of polyalcohols [37, 38] are also plotted in figure 7. The corresponding points are close to the dotted line. A similarity between the JG process of polyalcohols and the ν-process is expected. The hydroxyl group of polyalcohol

Table 1. The glass transition temperatures and loss peak frequencies at T_g, f_m ($T = T_g$) of the ν- and β-processes at various water mixtures plotted in figure 7.

| Solute | | $T_g(\tau_\alpha = 100 \text{ s})$ | f_m ($T = T_g$) (Hz) | |
Name	Conc. (wt%)	(K)	ν-process	β-process
2EG	65	154.5	2.57×10^{-1}	—[b]
3EG	65	161.8	7.38×10^{-1}	—[b]
4EG	65	168.1	2.49	—[b]
5EG	65	171.6	4.49	—[b]
6EG	65	174.0	8.00	—[b]
PEG400	65	178.4	1.13×10	—[b]
PEG600	65	178.4	9.01×10	—[b]
3EG	100	176.9	—[a]	8.04×10^2
	80	169.1	6.28×10^{-2}	—[b]
	70	164.2	3.84×10^{-1}	—[b]
	65	161.8	7.38×10^{-1}	—[b]
Glycerol	100	187.0	—[a]	—[b]
	80	170.0	2.33×10^{-1}	—[b]
	70	162.9	3.66×10^{-1}	—[b]
	60	156.6	1.18	—[b]
Ethylene glycol	80	144.9	6.05×10^{-3}	—[b]
	70	141.8	1.39×10^{-2}	—[b]
	60	138.7	7.69×10^{-2}	—[b]
Propanol	100	95.9	—[a]	1.99×10^2
	90	98.1	6.31×10^{-5}	2.40×10^2
	80	95.7	5.62×10^{-6}	1.07×10^2
Fructose	95	271.1	4.79×10^5	—[b]
	88	241.2	1.82×10^4	—[b]
	87	233.2	1.23×10^4	—[b]
	78	217.1	3.63×10^3	—[b]
	70	220.9	3.31×10^3	—[b]

[a] The ν-process does not appear.
[b] The β-process is unclear, since covered by other processes or limited frequency window of the measurement.

molecules has a dipole moment and the non-cooperative motion of polyalcohols is based on a kind of motion of hydroxyl groups. The molecular motion of water contributing to the ν-process is also some kind of motion of hydroxyl groups.

According to the above discussion, the high-frequency limit of the ν-process given by the dashed line in figure 7 is related to the crystallization of water in the mixture, while the low-frequency limit of the ν-process given by the dotted line in figure 7 seems to be related to the JG process of polyalcohols. Therefore, the ν-process appears to be an inherent molecular motion of water at subzero temperatures.

4. Conclusions

Two kinds of water exist in water mixtures with alcohol, ethylene glycol oligomers and fructose. One is excess water, which does not move cooperatively with solute molecules but has the inherent mobility of water molecules and is detected as the local ν-process. The other moves cooperatively with solute molecules and contributes to the α-process. Below T_S the ν-process

appears in the frequency range higher than the structural α-process, if the solute T_g is higher than that of pure water, and at a frequency lower than that of the α-process in the opposite case. The relaxation time of the ν-process is not strongly dependent on the structure and concentration of the solute and appears on a limited area of the Arrhenius plane. The strength of the ν-process decreases and that of the α-process increases with decreasing temperature, since the cooperativity of water and solute molecules increases with decreasing temperature.

The shape of the loss peak (asymmetric or symmetric) depends on the cooperative character of the relaxation of water and solute molecules, i.e. on whether the α-process or the ν-process is dominant in the liquid state. The separation below T_S of the α- and ν-processes for small-solute–water mixtures is the decoupling of the motions of excess water and solute molecules, whereas that for large-solute–water mixtures is the coupling of the motions of a part of the water molecules and the solute.

References

[1] Adachi K, Fujihara I and Ishida Y 1975 *J. Polym. Sci.* B **13** 2155
[2] Moynihan C T, Macedo P B, Montrose C J, Gupta P K, DeBolt M A, Dill J F, Dom B E, Drake P W,
 Easteal A J, Elterman P B, Moeller R P, Sasabe H and Wilder J A 1976 *Ann. N. Y. Acad. Sci.* **279** 15
[3] Schiener B and Böhmer R 1995 *J. Non-Cryst. Solids* **182** 180
[4] León C, Ngai K L and Roland C M 1999 *J. Chem. Phys.* **110** 11585
[5] Grzybowska K, Grzybowski A, Pawlus S, Hensel-Bielowka S and Paluch M 2005 *J. Chem. Phys.* **123** 204506
[6] Vogel H 1921 *Phys. Z.* **22** 645
[7] Fulcher G S 1923 *J. Am. Ceram. Soc.* **8** 339
[8] Davidson D W and Cole R H 1950 *J. Chem. Phys.* **18** 1417
[9] Kohlrausch R 1854 *Prog. Ann. Phys.* **91** 179
[10] Williams G and Watts D C 1971 *Trans. Faraday Soc.* **66** 80
[11] Cole K S and Cole R H 1941 *J. Chem. Phys.* **9** 341
[12] Ngai K L and Paluch M 2004 *J. Chem. Phys.* **120** 857
[13] Johari G P and Goldstein M 1970 *J. Chem. Phys.* **53** 2372
[14] Johari G P and Goldstein M 1971 *J. Chem. Phys.* **55** 4245
[15] Ngai K L 1998 *J. Chem. Phys.* **109** 6982
[16] Sudo S, Shinyashiki N and Yagihara S 2001 *J. Mol. Liq.* **90** 113
[17] Sudo S, Shimomura M, Shinyashiki N and Yagihara S 2002 *J. Non-Cryst. Solids* **307–310** 356
[18] Sudo S, Shimomura M, Saito T, Kashiwagi T, Shinyashiki N and Yagihara S 2002 *J. Non-Cryst. Solids* **305** 197
[19] Sudo S, Shimomura M, Tsubotani S, Shinyashiki N and Yagihara S 2004 *J. Chem. Phys.* **121** 7332
[20] Sudo S, Shimomura M, Kanari K, Shinyashiki N and Yagihara S 2006 *J. Chem. Phys.* **124** 044901
[21] Shinohara M, Goto T, Oyama M, Suzuki S, Shinyashiki N, Yagihara S, Inoue T, Oyaizu S and Yamamoto S 2006
 Proc. 2nd Int. Conf. on Flow Dynamics; *AIP Conf. Proc.* **832** 145
[22] Cerveny S, Schwartz G A, Alegria A, Bergman R and Swenson J 2006 *J. Chem. Phys.* **124** 194501
[23] Tyagi M and Murthy S S N 2006 *Carbohydr. Res.* **341** 650
[24] Sudo S, Tobinai S, Shinyashiki N and Yagihara S 2006 *Proc. 2nd Int. Conf. on Flow Dynamics*; *AIP Conf. Proc.*
 832 149
[25] Casalini R and Roland C M 2004 *Phys. Rev.* E **69** 094202
[26] Adam G and Gibbs J H 1965 *J. Chem. Phys.* **43** 139
[27] Shinyashiki N, Sudo S, Abe W and Yagihara S 1998 *J. Chem. Phys.* **109** 9843
[28] Johari G P 2005 *J. Chem. Phys.* **122** 144508
[29] Pathmanathan K and Johari G P 1990 *J. Polym. Sci. Polym. Phys.* B **28** 675
[30] Pathmanathan K and Johari G P 1994 *J. Chem. Soc. Faraday Trans.* **90** 1143
[31] Xu H, Vij J K and McBrierty V J 1994 *Polymer* **35** 227
[32] Bergman R and Swenson J 2000 *Nature* **403** 283
[33] Buchner R, Barthel J and Stauber J 1999 *Chem. Phys. Lett.* **306** 57
[34] Ngai K L and Capaccioli S 2004 *J. Phys. Chem.* B **108** 11118
[35] Böhmer R, Ngai K L, Angell C A and Plazek D J 1993 *J. Chem. Phys.* **99** 4201
[36] Ngai K L and Tsang K Y 1999 *Phys. Rev.* E **60** 4511
[37] Döß A, Paluch M, Sillescu H and Hinze G 2002 *Phys. Rev. Lett.* **88** 095701
[38] Ngai K L, Lunkenheimer P, León C, Schneider U, Brand R and Loidl A 2001 *J. Chem. Phys.* **115** 1405